Comparative study of electric and hydrogen mobility infrastructures for sustainable public transport: A PyPSA optimization for a remote island context

International Journal of Hydrogen Energy 80 (2024) 516–527

Contents lists available at ScienceDirect

International Journal of Hydrogen Energy

journal homepage: www.elsevier.com/locate/he

Comparative study of electric and hydrogen mobility infrastructures for sustainable public transport: A PyPSA optimization for a remote island context

Elena Rozzi [a,c,*], Enrico Giglio [b,c,d], Claudio Moscoloni [d,e], Riccardo Novo [b,d], Giuliana Mattiazzo [b,c,d], Andrea Lanzini [a,c]

[a] Department of Energy, Politecnico di Torino, Corso Duca degli Abruzzi 24, 10129, Torino, Italy
[b] Department of Mechanical and Aerospace Engineering, Politecnico di Torino, Corso Duca degli Abruzzi 24, 10129, Torino, Italy
[c] Energy Center Lab, Politecnico di Torino, Via Paolo Borsellino 38/16, 10138, Torino, Italy
[d] Marine Offshore Renewable Energy Lab (MOREnergy Lab, Politecnico di Torino, Via Paolo Borsellino 38/16, 10138, Torino, Italy
[e] STS Class Scuola, Istituto Universitario di Studi Superiori IUSS di Pavia, Piazza della Vittoria 15, 271000, Pavia, Italy

ARTICLE INFO

Keywords:
BEV
FCEV
PyPSA
Road transportation
Electric mobility

ABSTRACT

Decarbonizing road transportation is vital for addressing climate change, given that the sector currently contributes to 16% of global GHG emissions. This paper presents a comparative analysis of electric and hydrogen mobility infrastructures in a remote context, i.e., an off-grid island. The assessment includes resource assessment and sizing of renewable energy power plants to facilitate on-site self-production. We introduce a comprehensive methodology for sizing the overall infrastructure and carry out a set of techno-economic simulations to optimize both energy performance and cost-effectiveness. The levelized cost of driving at the hydrogen refueling station is 0.40 €/km, i.e., 20% lower than the electric charging station. However, when considering the total annualized cost, the battery-electric scenario (110 k€/year) is more favorable compared to the hydrogen scenario (170 k€/year). To facilitate informed decision-making, we employ a multi-criteria decision-making analysis to navigate through the techno-economic findings. When considering a combination of economic and environmental criteria, the hydrogen mobility infrastructure emerges as the preferred solution. However, when energy efficiency is taken into account, electric mobility proves to be more advantageous.

1. Introduction

Decarbonizing road transportation is a pivotal measure in achieving long-term goals for mitigating climate change. Indeed, the road transport sector accounts for 16% of global emissions [1]. In 2023, the European Council embraced a new regulation that establishes more rigorous targets for reducing CO_2 emissions. This regulation also includes a ban on the sale of new passenger and light commercial vehicles that emit CO_2 after 2035.

The electric mobility infrastructure is simpler and more mature compared to hydrogen-based infrastructure. Battery-electric vehicles (BEVs) utilize rechargeable batteries in combination with one or multiple motors [2]. The average range of BEVs typically falls between 100 and 350 km, with some models capable of reaching up to 1000 km on a single charge [3]. The market for BEVs and plug-in hybrid electric vehicles is experiencing rapid expansion, with a remarkable result of 6.6 million cars sold in 2021. This figure accounts for approximately 9% of the global car market [4].

Several factors have contributed to the surge in the electric car market, including significant improvements in the driving range and performance of electric vehicles, as well as the growing availability of fast charging stations [5]. In 2021, the number of publicly available fast-charging stations reached 570,000 globally, with a growth rate close to 45% [1].

Moreover, there were 700,000 electric buses on the road worldwide in 2022, with China leading the way at 95% of the total. In Europe, 14,000 buses were electric, comprising 0.9% of the market share. Projections indicate that this share will rise to 4% in 2025 and 13%–18% in 2030 [6].

Fuel-cell electric vehicles (FCEVs) are similar to BEVs. However, they have a fuel cell powered by hydrogen that generates electricity. The typical hydrogen consumption is 0.76–1 kg_{H_2}/100 km and the tank stores about 5–6 kg of hydrogen fuel [7].

The market for FCEVs is less developed compared to BEVs. As of 2021, there were 51,600 FCEVs worldwide, with 67% of them located

* Corresponding author at: Energy Center Lab, Politecnico di Torino, Via Paolo Borsellino 38/16, 10138, Torino, Italy.
E-mail address: elena.rozzi@polito.it (E. Rozzi).

https://doi.org/10.1016/j.ijhydene.2024.07.105
Received 11 January 2024; Received in revised form 3 July 2024; Accepted 8 July 2024
Available online 17 July 2024
0360-3199/

Abbreviations

BEC	Bare Erected Cost
BESS	Battery Energy Storage System
BEVs	Battery Electric Vehicles
CAPEX	Capital Cost
CRITIC	Criteria Importance Trough Intercriteria Correlation
DW	Deionized Water
EPCC	Engineering, Procurement and Construction Cost
EV	Electric Vehicle
FCEVs	Fuel-Cell Electric Vehicles
HP	High Pressure
HRS	Hydrogen Refueling Station
LCOD	Levelized Cost of Driving
LCOM	Levelized Cost of Mobility
LP	Low Pressure
MCDM	Multicriteria Decision Making Analysis
OPEX	Operational Cost
PEM	Proton Exchange Membrane
PMS	Power Management Strategy
PV	Photovoltaic
RES	Renewable Energy Source
SEBE	Solar Energy on Buildings Envelopes
TAC	total Annualized Cost
TOC	Total Overnight Cost
TOPSIS	Technique for Order of Preference by Similarity to Ideal Solution
WAsP	Wind Atlas Analysis and Application Program
ZLEVs	Zero- and Low-Emissions Vehicles

Parameters

A^+, A^-	Alternatives (+)best (−)worst
C_j	Decision criteria
DL_g^{static}	Daily load on the gth day
E_{ac}	Annual producibility
G_{STC}	Irradiance in standard test conditions
H_g	Average global irradiance
i	Nominal interest rate
LF	Levelizetion factor
$l_g^{opt}(h)$	Charging load at the hth hour of the gth day
m	Number of evaluation criteria
M_{H_2}	Molecular mass of hydrogen
N	Number of compressor stages
n	Lifetime
P_N	Nominal power
PR	Performance ratio
Q	Flow rate
R	Ideal gas constante
r_{jk}	Correlation term
$S_i^{\pm}$	Euclidean distance (+)best (−)worst
$s_{l,g}^{opt}(h)$	Status of the load
V_i	Closeness index
v_j	Weighted normalized performance
w_j	Objective weights
x_j	Performance of evaluation criteria
Z	Compressibility factor
η	Efficiency
γ	Diatomic constant factor
σ_j	Divergence index of the scores

in Asia, and only 730 hydrogen refueling stations (HRS) installed globally [8]. The majority of FCEVs (around 85%) are passenger light-duty vehicles, while the remaining portion is divided equally between buses and heavy-duty trucks [9]. Projections from the International Energy Agency [10] suggest that by 2030, in the Sustainable Development Scenario, electric vehicles will make up 41% of total car and light truck sales, with FCEVs accounting for only 1%.

Although the market for FCEVs is less developed compared to BEVs, hydrogen-powered vehicles have significant potential due to hydrogen's higher energy density in terms of both weight and volume [11].

Moreover, the current limitation for FCEVs lies in the infrastructure, which is still constrained by the shortage of HRS in operation. However, HRS offers several advantages. One key benefit is the remarkably fast charging time, ranging from 5 to 15 min [12], compared to BEVs, which typically require from 4–8 h (slow charging) to 20–30 min (fast charging) to reach 80% of their state of charge [13].

Finally, the Hydrogen Roadmap Europe [14] compares the CO_2 well-to-wheel emissions across different powertrains (excluding manufacturing) showing that both BEVs and FCEVs are less CO_2 intensive than internal combustion engines vehicles powered by diesel or gasoline. FCEVs powered by green hydrogen generate about 15 g_{CO_2}/km, while hydrogen produced by steam methane reforming emits around 75 g_{CO_2}/km. The BEVs' emissions range from 10 to 55 g_{CO_2}/km depending on the electricity source. However, when considering emissions from manufacturing processes, FCEVs become more advantageous than BEVs, as fuel cells are less energy-intensive to produce than batteries.

1.1. Literature review

While several optimization studies have been conducted on BEV charging infrastructure, as reported in the review paper by Shen et al. [15], fewer studies focus on optimizing the size of HRS.

Shen et al. [15] conducted a comprehensive review of BEV charging infrastructure, covering key characteristics of the EV industry, strategies for planning and optimizing EV charging infrastructure operations, and an analysis of the roles and potentials of public policies and business models.

Verzijlbergh et al. [16] investigated the potential of electric vehicles to support high penetration of renewable energy generation on a small island in Portugal. The optimal charge policies of the EV fleet were defined using a dynamic programming algorithm.

The optimization of a microgrid design with electric vehicle charging stations powered by photovoltaic panels is proposed by Işik et al. [17]. The objective of this study is the optimal sizing and scheduling of the electric vehicle charging stations, PV panels, and battery storage systems to minimize energy costs and carbon emissions using the HOMER simulation tool.

Nafeh et al. [18] presented an optimization problem for sizing a PV-battery grid-connected system for fast charging stations for electric vehicles, comparing five meta-heuristic optimization algorithms. They also developed a novel rule-based energy management strategy based on two pricing strategies, achieving a levelized cost of energy ranging from 0.051 to 0.071 $/kWh.

Similarly, the optimization of wind power and HRS sizing and operation to reduce costs and emissions is proposed by Zhao et al. [19], while Barhoumi et al. [20] developed a model for the optimization of a grid-connected PV system for hydrogen production used in refueling FCEVs, estimating the levelized cost of hydrogen production at 4.2 €/kg with an average production of 400 kg/day. Barhoumi et al. [21]

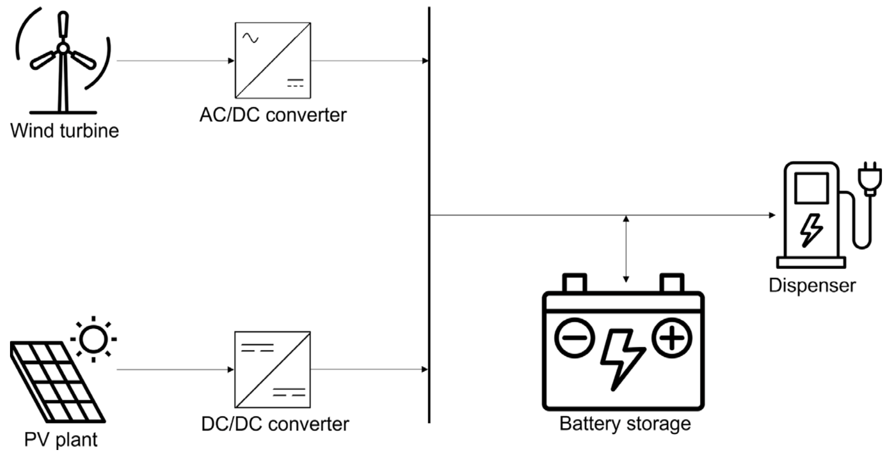

Fig. 1. Schematic of the electric mobility infrastructure.

also conducted a techno-economic optimization of hydrogen production for refueling FCEVs using wind energy within three scenarios: The levelized cost of hydrogen ranges from 6.24 €/kg for the grid-connected scenario to 14.2 €/kg for the configuration with a fuel cell backup unit due to the high investment cost of fuel cells and batteries that are not competitive with electricity costs from the grid.

Moreover, Ibáñez-Rioja et al. [22] analyzed the optimization of system control and component capacities for a green hydrogen production system powered by an off-grid PV-wind plant integrated with a battery energy storage system (BESS) over 30 years in Finland. The model was optimized using a particle swarm optimization algorithm to minimize the levelized cost of hydrogen. The results indicate that the battery was introduced in the optimal scenario only after 2035, and the PV plant after 2040. The levelized cost of hydrogen ranged from 1.72 €/kg in 2040 to 2.34 €/kg in 2020, but it is worth noting that this analysis did not include the HRS.

Schröder et al. [23] explored the simultaneous optimization of distributed energy resources, component sizes, and energy management strategies to minimize the costs of BEVs charging and FCEVs refueling using a genetic algorithm. Their results indicate that using battery energy storage for peak shaving can minimize the overall costs of distributed energy resources and reduce their dependence on the utility grid.

Additionally, an assessment of a HRS powered by surplus energy from a 10 MW wind farm, as detailed by Kavadias et al. [24], indicated that it could indeed be a viable solution when designed appropriately. The economic viability of such a station was found to improve with a higher penetration of FCEVs.

Furthermore, Wu et al. [25] presented a multi-stage stochastic programming model designed to determine the optimal approach for providing HRS services within energy and reserve markets. They considered various scenarios representing uncertainties related to day-ahead prices, reserve prices, system imbalance prices, and hydrogen demand, all aimed at maximizing expected profits.

Finally, the comprehensive assessment of the economic viability of a HRS [26] took into account the capacities of 100 kg/day and 1000 kg/day and estimated the levelized cost of hydrogen to be between 7.7 and 6.8 $/kg, respectively. However, the real cost of hydrogen depends on the production system performance and utilization factor [27]. While the economic model of hydrogen infrastructure developed by Brown et al. [28] showed that the LCOD of fuel cell vehicles can be lower than equivalent gasoline internal combustion engine vehicles in the near and long term.

Our research identifies a significant gap in the literature concerning the optimization of HRS sizing and operation. This gap involves the integration of resource assessment, renewable power plant sizing, and HRS infrastructure optimization. It is worth noting that many existing studies tend to focus on a single evaluation criterion, such as the minimization of investment cost or the levelized cost of energy, whereas the comprehensive assessment of infrastructure performance should encompass both techno-economic and environmental parameters.

1.2. Novelty and contribution

To address the identified gap, we aim to provide a comprehensive methodology for the techno-economic assessment and optimization of HRS. We apply this methodology to a case study aimed at comparing two public transport infrastructures, electric and hydrogen, on Pantelleria Island, in Italy.

This study encompasses the resource assessment and sizing of two renewable energy power plants – a building integrated PV system, and a small wind turbine – located near the new National Park headquarters to enable on-site production of electricity or hydrogen. The techno-economic simulations and optimization of the overall infrastructure sizing are performed using PyPSA [29] to find the optimal compromise between performance and costs, while meeting energy demand.

Moreover, as previously mentioned, the decarbonization of the public transport sector appears crucial in achieving the long-term decarbonization target, as envisaged by Danielis et al. [30]. To navigate the techno-economic results, a Multicriteria Decision Making Analysis (MDMA), supported by a hybrid multicriteria analysis based on the TOPSIS method [31] and CRITIC one [32], has been performed considering techno-economic and environmental parameters. To the extent of our knowledge, no previous work has adopted a similar approach to optimize the size of HRS.

Section 2 describes the methodology for the resource assessment, the optimization model, and techno-economic evaluations. Section 3 introduces the case study of Pantelleria Island, whereas Section 4 presents the results and discussion. Finally, Section 5 draws conclusions.

2. Methods

The plant configurations analyzed encompass electricity generation from renewable sources, hydrogen production for FCEVs, as well as electricity or hydrogen storage, and energy dispensing for vehicle refueling.

The BEVs infrastructure (Fig. 1) is straightforward and well-established: electricity is generated by photovoltaic and wind power plants, stored in lithium-ion batteries, and dispensed through fast charging stations.

On the other hand, the HRS involves a more complex setup (Fig. 2). The electricity generated by photovoltaic and wind power plants undergoes electrolysis to produce hydrogen, which is then stored in a low-pressure buffer tank. Hydrogen is then compressed and stored in

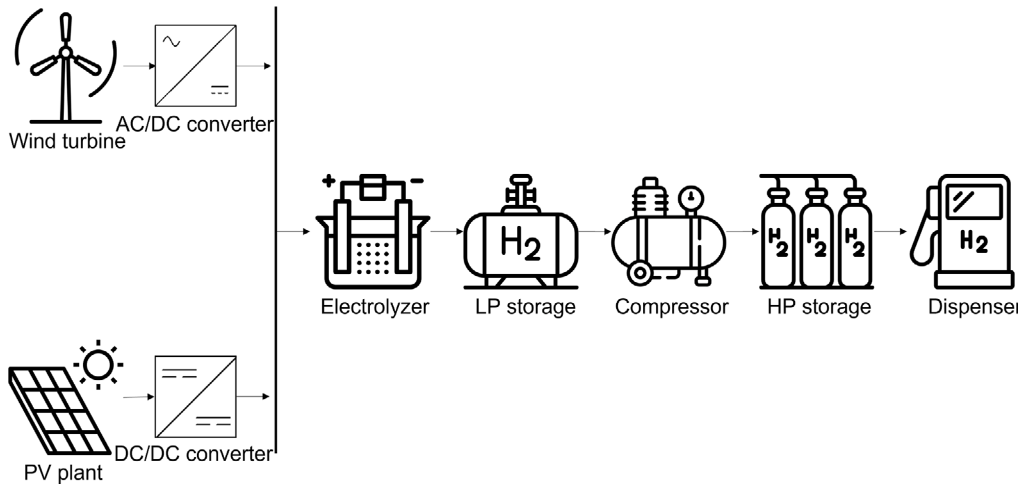

Fig. 2. Schematic of the hydrogen mobility infrastructure.

high-pressure cascade tanks. Finally, hydrogen is dispensed to refuel the vehicles [33,34]. The low-pressure storage serves as a buffer between the electrolyzer's output and the hydrogen compression unit. The cascade storage system is introduced as it could reduce energy consumption, increase the filling speed, and reduce operating cost [35].

2.1. Renewable energy production

An assessment of the solar and wind resources availability was carried out to evaluate the feasibility and optimal size of photovoltaic and wind power plants.

To determine the potential solar resource on the selected site, the Solar Energy on Buildings Envelopes (SEBE) [36] plugin for QGIS [37] was used [38]. This plugin operates alongside the Urban Multi-scale Environmental Predictor tool [39], which provides essential input data, including the Digital Surface Model for buildings and ground, meteorological data, albedo, wall height, and wall aspect (angle) raster. The SEBE plugin calculates the solar irradiance at a pixel resolution of 2 m, and the average of pixel values provides the solar irradiance on the chosen surface. The maximum number of photovoltaic modules that can be installed on a pitch was evaluated using AutoCAD software [40], with the single module size sourced from the manufacturer's datasheet.

With this information, the maximum annual energy producibility of the photovoltaic system is computed (Eq. (1)):

$$E_{ac} = P_N \cdot H_g / G_{STC} \cdot PR \tag{1}$$

Where P_N is the peak power of the installed photovoltaic plant, H_g is the average global irradiance, G_{STC} is the irradiance in standard test condition, and PR is the performance ratio which accounts for the efficiency losses of the PV plant. To determine the hourly and daily production profile for a case-study PV plant, we scaled the annual producibility with hourly and daily production data from PVGIS [41].

The WAsP (Wind Atlas Analysis and Application Program) [42] software was utilized for the wind resource assessment, site selection, and energy yield calculations concerning wind turbines. By importing data from the Global Wind Atlas, WAsP integrates flow models that account for orography, surface roughness, roughness change effects, and obstacle influences. The output provides precise information regarding wind turbine locations, including elevation, mean wind speed, mean power density, ruggedness index, and Weibull values, and assesses annual energy production and potential energy yield for wind power projects. Furthermore, by incorporating the power curve of the selected turbines into WAsP, the annual energy production is calculated. Subsequently, the annual production is scaled based on hourly and daily production data from Renewables.ninja [43].

2.2. Modeling and optimization in PyPSA

The two plant configurations – hydrogen and electric mobility infrastructure – are modeled in the PyPSA framework [29]. The model is solved using the CPLEX solver V20.1.1 [44] on a machine equipped with an AMD Ryzen 9 3900X processor and 64 GB of RAM. The simulations are performed for an entire year, with hourly time-step and a maximum gap tolerance equals to $10^{-4}\%$. The goal of this optimization is to minimize the total annualized cost of the modeled systems, including capital ($CAPEX_{tot}$) and operational expenses ($OPEX_{tot}$), as described in Eq. (2). The optimal sizes of the key components and the power management strategy (PMS) are determined. The PMS outlines the temporal sequence of production, storage, and refueling activities, thereby defining the power consumption for each time step.

$$\min f_{obj}^{base} = \min \left\{ CAPEX_{tot} + OPEX_{tot} \right\} \tag{2}$$

2.2.1. Hydrogen mobility infrastructure

Energy generated by the photovoltaic and wind plants is converted into hydrogen through water electrolysis. The electrolyzer and compressor nominal power, the buffer, and the cascade storage volumes are optimized through PyPSA. The model features a central node to which the plant components are connected (Fig. 3): two generators (PV and wind power plants), two storage nodes (buffer and cascade), and a load representing the demand of buses. The electrolyzer and the compressor establish the link between the storage unit and the central node. The electrolyzer and compressor efficiencies are assumed to be constant at their nominal values and are 65% and 75%, respectively.

The power consumption for compression is evaluated according to equation (Eq. (3)):

$$P = Q \cdot \frac{Z \cdot T \cdot R}{M_{H_2} \cdot \eta_{comp}} \cdot \frac{N \cdot \gamma}{\gamma - 1} \cdot \left[\frac{P_{out}}{P_{in}}^{\frac{\gamma-1}{N \cdot \gamma}} - 1 \right] \tag{3}$$

Where Q is the flow rate, Z is the hydrogen compressibility factor, T is the inlet temperature of the compressor, R is the ideal gas constant, M_{H_2} is the molecular mass of hydrogen, η the compression efficiency, N the number of compressor stages, and γ the diatomic constant factor.

In addition to the scenario described above, we conducted another simulation where the load profile was not pre-defined; rather, the hours during which buses were recharged were also optimized. Specifically, two constraints were introduced: firstly, to maintain the daily load demand unchanged compared to the static case, and secondly, to ensure a consistent 2-h total charging period. These aspects were implemented by introducing Eqs. (4) and (5). Here, DL_g^{static} represents the daily load

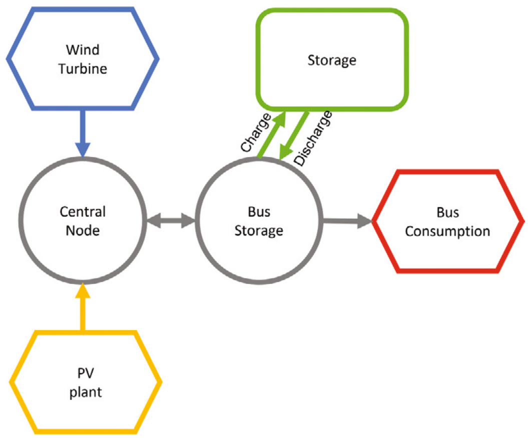

Fig. 3. Schematic of the mobility infrastructure modeled in PyPSA.

on the gth day of the year, $l_g^{opt}(h)$ represents the charging load at the hth hour of the gth day of the year, and $s_{l,g}^{opt}(h)$ represents the status of the load (a binary variable, equal to 1 during bus charging). These latter two variables are now being optimized, in contrast to the previous simulation where they were given as input.

$$DL_g^{static} = \sum_{h=1}^{24} l_g^{opt}(h) \tag{4}$$

$$\sum_{h=1}^{24} s_{l,g}^{opt}(h) \leq 2 \tag{5}$$

2.2.2. Electric mobility infrastructure

The nominal power and capacity of the electrochemical storage are optimized in PyPSA. The model structure closely resembles the model described for the hydrogen infrastructure. In this configuration, the battery charge and discharge mechanisms work as a link connecting the storage to the central node. The round-trip efficiency of the battery has been considered equal to 90%, equally divided between charge and discharge, and the state of charge has been assumed to be balanced.

2.3. Techno-economic evaluation

The economic viability of the two mobility infrastructures is assessed by evaluating the total annualized costs (TAC) and the levelized cost of driving (LCOD). The levelized cost of driving (LCOD) is evaluated by multiplying the levelized cost of hydrogen or battery mobility infrastructure (LCOM) with the specific fuel consumption by the vehicle. The levelized cost of mobility (Eq. (6)) is estimated as a function of the total overnight cost (TOC) of the components, which encompass capital cost (CAPEX) and overnight costs [45] including the expenses for both production and refueling infrastructures, fixed (OPEX_{fix}) and variable(OPEX_{var}) operational and maintenance costs, annual revenues obtained by selling the electricity excess from the RES power plant, and the net energy output (hydrogen or electricity) supplied for vehicles refueling (Energy) [46].

$$LCOM = \frac{LF \cdot TOC + OPEX_{fix} + OPEX_{var} - Revenues}{Energy} \tag{6}$$

LF denotes the levelization factor, which takes into account the plant lifetime (n) and the nominal interest rate (i):

$$LF = \frac{i \cdot (1+i)^n}{(1+i)^n - 1} \tag{7}$$

2.4. Multicriteria decision-making analysis

Developing a sustainable mobility project involves technical, economic, and social aspects imposing a broader perspective from the decision-makers in the planning, analysis, and decision phase, as pointed out by Broniewwicz and Ogrodnik [47].

In such a complex environment, encompassing each aspect as much as possible appears crucial. The multi-criteria decision-making analysis supports the development of a sustainable transport strategy by enclosing the different performance indices and analyzing the mutual relationship between them.

Broniewicz et al. [48] analyze the relatively young multicriteria decision analysis panorama, comparing several methods evaluating the strengths and weakness of each approach in sustainable transport applications; moreover, the authors found an evident trend concerning the transparency, integration, and versatility of the algorithms investigated, that depicts a broad application of the TOPSIS family in the analysis of sustainable transport problems.

In light of this, the scenarios' outcomes are assessed by proposing a hybrid multicriteria analysis mainly based on the TOPSIS method, where the objective weights have been derived by integrating the CRITIC method.

The proposed hybrid technique encompasses the CRITIC method, a well-established weighting technique that provides the weights of the evaluation criteria in a multicriteria problem, measuring the contrast and the conflict between each performance index applying a correlation analysis, as presented, for instance, by Hassan et al. [49].

Within this work, the TOPSIS method introduces the decision aspect, implementing a decision criterion based on the closeness, i.e. the Euclidean distance, of the investigated solution, weighted through the CRITIC results, with respect to the identified best ideal solution.

2.4.1. CRITIC

The objective weights calculation, according to the CRITIC method, foresees the definition of the multicriteria problem as a set of A alternatives evaluated through m evaluation criteria. The relative score matrix x_j measures the performance of each alternative concerning each evaluation criterion, has been built performing a mapping function x_{aj} that expresses the normalized Euclidean distance from the ideal solution.

The introduction of the parameter C_j depicts the contrast and the conflict of each decision criterion that, according to Mukhametzyanov [50] and Diakoulaki [32], represents the quantity of information conveyed by the MCDM problem concerning a single evaluation criterion.

$$C_j = \sigma_j \sum_{k=1}^{m} (1 - r_{jk}) \tag{8}$$

Where σ_j is a divergence index of the scores, and r_{jk} is the correlation term. By normalization of the Eq. (8), the objective weights w_j are obtained.

$$w_j = \frac{C_j}{\sum_{k=1}^{m} (C_k)} \tag{9}$$

2.4.2. TOPSIS

The decision analysis has been performed by means of the TOPSIS method, developed by Hwang [31], which states that the best solution is the nearest to the positive ideal solution. The alternatives have been ranked according to the previous criterion.

The relative score matrix x_j has been normalized by means of its norm in order to perform a comparison of dimensionless attributes; moreover, each normalized performance score has been weighted using the CRITIC's weights obtained by means to the Eq. (9), as follows:

$$v_{ij} = \frac{x_{ij}}{\sqrt{\sum_{i=1}^{N} x_{ij}^2}} \times w_j \tag{10}$$

Obtained the weighted normalized performance matrix, pointed out as v_{ij}, A^+ and A^- denote respectively the best performance value and the worst one for each evaluation criterion, as highlighted by Chakraborty [51], and reported as follows:

$$A^+ = [v_1^+, v_2^+, \dots, v_J^+,] \tag{11}$$

$$A^- = [v_1^-, v_2^-, \dots, v_J^-,] \tag{12}$$

In which, for each evaluation criterion, v_j^+ corresponds to the $max(v_{ij})$ if it is related to a positive performance; otherwise, it corresponds to the $min(v_{ij})$. Likewise, v_j^- corresponds to the $min(v_{ij})$ if it is related to a positive performance; elseways, it corresponds to the $max(v_{ij})$

The separation measure $S_i^{\pm}$ is the Euclidean distance of each relative performance score from, respectively, the best and the worst ideal solution. Adopting a closeness index V_i as an overall preference score, the ranking of the alternatives is obtained based on a higher value of V_i.

$$V_i = \frac{S^-}{S^+ + S^-} \tag{13}$$

3. Case study: Pantelleria Island

Pantelleria is a Mediterranean island that spans over 80 km^2, located 100 km southwest of Sicily, Italy. The Pantelleria National Park encompasses 80% of the entire land area. The island's redevelopment project aims to repurpose part of the military area in Bukkuram into the new National Park headquarters and generate electricity through renewable energy sources while implementing modern public transportation infrastructure. An energy model for Pantelleria Island, combining the adoption trends of distributed photovoltaic systems and electric vehicles, was developed by Novo et al. [52].

3.1. Public transport

The public transportation system comprises five bus routes that interconnect key points of interest with the central area of the Pantelleria municipality [53]. The public transportation system operates with a fleet of seven mini-buses. The distance covered by these mini-busses each day varies based on the season and holidays. On summer weekdays, the traveled distance amounts to 610 km per day, which decreases to 450 km per day during summer holidays. Throughout the winter period (from September to June), the mini-buses cover a daily distance of 600 km and the urban transport service does not operate on Sundays. As the longest route traveled by mini-buses is 240 km, the refueling process occurs once per day.

The hydrogen consumption of fuel cell mini-buses is 6.6 kg/100 km. Hydrogen is stored within a 16.5 kg storage tank pressurized at 350 bar, providing an autonomy of 250 km [54,55]. This results in an average daily hydrogen consumption of 40 kg (1330 kWh based on hydrogen lower heating value).

Similarly, battery-electric mini-buses exhibit a 250-kilometer range and an approximate energy consumption of 1.1 kWh/km [56]. The average daily electric consumption reaches 605 kWh, with a maximum of 610 kWh observed during summer days.

Overall, the annual hydrogen consumption amounts to 12 545 kg (420 MWh), while the annual electric consumption stands at 220 MWh.

The assumptions related to the public transportation system and the buses' consumption are summarized in Table 1.

3.2. Renewable energy production and sizing

The photovoltaic plant is placed on the rooftop of the National Park headquarters, comprising 18 pitches. The average solar irradiation on each pitch is evaluated according to the methodology outlined in Section 2.1. Employing monocrystalline PV modules with a peak power of 480 W, boasting an efficiency of 21%, and occupying an area of 2.25 m^2 each [58], the number of modules that can be installed on a single pitch is 12, resulting in a maximum installable capacity of 104 kWp. Therefore, the maximum annual producibility of the plant (Eq. (1)) approximates 160 MWh. The size of the PV plant is optimized in PyPSA. The total overnight costs for the photovoltaic plant are 1750 €/kW [59,60], the lifetime reaches 30 years [60,61], and the operational and maintenance costs are 1.3% of CAPEX [60,62].

Regarding wind energy, just a small turbine can be installed in this area, due to the regulatory limitation on large wind turbines in force in Pantelleria [38]. The nominal power of the reference wind turbine is 100 kW, and the effective size is selected by the optimization model. The turbine is placed following criteria of space and producibility in the northernmost and highest position on the National Park hill, as suggested by the WAsP software. The annual energy production of the reference wind turbine stands at around 1200 MWh. The total overnight cost for the wind turbine installation is 3000 €/kW [60], the plant lifetime is 30 years [60,63], and the OPEX costs are 1% of CAPEX [59,60].

3.3. Hydrogen mobility infrastructure

In the hydrogen infrastructure, the electricity generated by photovoltaic and wind power plants is converted into hydrogen through water electrolysis. A proton exchange membrane (PEM) electrolyzer is supplied with deionized water (DW), which is split into oxygen and hydrogen. The outlet pressure of the resulting hydrogen is 30 bar.

Techno-economic parameters of the PEM electrolyzer are summarized in Table 2. The total investment cost for the electrolyzer is approximately 2450 €/kW [64].

The low-pressure storage operates at a maximum pressure of 30 bar, avoiding the need for an additional compressor [33]. The compression

Table 1
Public transport features.

Feature	Values	Refs
	Public transport	
Number of routes	5	[53]
Number of buses	7	[53]
km traveled per day	Winter: 600 km/d Summer weekdays: 610 km/d Summer holidays: 450 km/d	[53]
Longest travel per day	240 km/d	[53]
	Hydrogen-powered buses	
H_2 consumption	6.6 kg/100 km 2.2 kWh/km (LHV)	[54,55]
H_2 capacity	16.5 kg @350 bar	[57]
Autonomy	250 km	[57]
	Battery-powered buses	
Electric consumption	1.1 kWh/km	[56]
Battery capacity	250 kWh	[56]
Autonomy	250 km	[56]

Table 2
Techno-economic parameters of a PEM electrolyzer.

	Values	Refs
Energy efficiency	65%	[65,66]
Operational temperature	50–80 °C	[65,66]
Operational pressure (inlet–outlet)	1 bar–30 bar	[65,66]
Operational range	5%–100%	[65,66]
Deionized water consumption	9 l/kg$_{H_2}$	[66,67]
CAPEX	1750 €/kW	[65,68]
OPEX fix	6%CAPEX[a]	[65,68]
OPEX variable (DW)	0.01 €/kg$_{H_2}$	[67,69]
Lifetime	10–15 years	[65,70]

[a] Encompasses the electrolyzer replacement cost (30%–40% of CAPEX) spread over the lifetime.

Table 3
Techno-economic parameters of auxiliary components in the hydrogen infrastructure.

	TOC	OPEX[a]	Lifetime	Operating range	Refs
LP storage	100 €/m^3	2.5%	20–30 yr	0–173 bar	[72,73]
HP storage	130 €/m^3	2.5%	20–30 yr	300–510 bar	[72,73]
Compressor	2300 €/kW	5%	10–20 yr	30–500 bar	[72,74]
H_2 dispenser	45,000 €	2%	10–20 yr	50 kg/day	[72,74]

[a] Fixed operational and maintenance costs expressed as %CAPEX.

Table 4
Techno-economic parameters of Lithium-ion storage battery.

	Values	Refs
Energy efficiency	85%	[78,79]
Operational temperature	25 °C	[79]
Operational range	10%–90%	[79]
Self-discharge rate	0.1%–0.3%	[78]
CAPEX	300 €/kWh + 180 €/kW	[80]
OPEX fix	6 €/kWh + 18 €/kW	[80]
OPEX variable	0 €/MWh	[60]
Lifetime	5–15 years	[78]

Encompasses the battery replacement cost (30%–40% of CAPEX) spread over the lifetime.

unit raises the pressure from 30 to 500 bar, which corresponds to the maximum pressure of the high-pressure storage [71]. The overall compression efficiency is assumed to be 75%, and the number of stages is set to 2 [66]. With these assumptions, the energy losses due to compression, calculated as a percentage of the lower heating value (LHV), are approximately 8%.

Hydrogen is dispensed using a dedicated dispenser at a pressure of 350 bar, which matches the storage pressure of the buses. The initial hydrogen level in the storage tank is assumed to be 50% of its total capacity.

Techno-economic characteristics of auxiliary components within the hydrogen infrastructure are outlined in Table 3.

The refueling process for each bus takes around 10-15 min [75] and can only occur once per day, to maximize the availability of the buses for the public transport service.

Finally, the remuneration of the electricity injected into the electric grid is established at 0.14 €/kWh [76,77], and the nominal interest rate is set equal to 4%.

3.4. Battery-electric mobility infrastructure

In the context of electric mobility infrastructure, the central element is the lithium-ion storage battery. Table 4 outlines the techno-economic parameters of the storage battery.

The initial state of charge of the BESS is assumed to be 50% of its total capacity.

With a fleet of seven buses and a 150-kW dispenser, an individual full charge duration lasts 1.4 h, and the complete fleet can be recharged within a ten-hour time frame.

The CAPEX of the dispenser is set at 95,000 €, with fixed OPEX accounting for 2% of the CAPEX [81]. The expected operational lifetime typically ranges from 10 to 20 years.

4. Results and discussion

In this study, we investigate three distinct scenarios related to the infrastructure for refueling stations catering to electric and hydrogen vehicles:

1. hydrogen mobility with a pre-defined load profile denoted as H_2LoadSet;
2. hydrogen mobility with optimized bus recharge time slots, denoted as H_2LoadOpt;
3. electric mobility with a pre-defined load profile denoted as EVLoadSet.

Table 5
Energy balance summary for the three scenarios: EVLoadSet, H_2LoadSet, and H_2LoadOpt.

	Bus energy	Delivered energy	RES prod.	RES to load	RES to grid
EVLoadSet	190	220	387	293	94
H_2LoadSet	190	420	1398	704	694
H_2LoadOpt	190	420	1398	704	694

Table 6
Efficiencies, self-consumption, and self-sufficiency metrics for the three scenarios: EVLoadSet, H_2LoadSet, and H_2LoadOpt.

	Well-to-Vehicle efficiency	Well-to-Wheels efficiency	Self-cons.	Self-suff.
EVLoadSet	75%	65%	76%	100%
H_2LoadSet	60%	27%	50%	100%
H_2LoadOpt	60%	27%	50%	100%

As summarized in Tables 5 and 6, the total energy generation required to meet the load (RES to load) is 704 MWh for the H_2LoadSet and H_2LoadOpt scenarios, compared to 293 MWh for the EVLoadSet case. The bus electricity consumption (Bus energy) represents the energy used by the vehicle, where fuel is processed to provide power, amounting to 190 MWh in all scenarios. The energy delivered to the bus (Delivered energy), which depends on the conversion efficiency of the bus engine, is 220 MWh for the EVLoadSet case (battery round-trip efficiency of 85%) and 420 MWh for the H_2LoadSet and H_2LoadOpt scenarios, where the fuel cell operates at 50% efficiency.

The total energy generation (RES prod.) is sized to meet the load demand at every timestep of the year, thus exceeding the electricity delivered to the load and including the electricity injected into the grid (RES to grid). In the H_2Load scenarios, the total electricity generated is almost double the electricity delivered to the load, due to the oversizing of the wind plant to always meet the demand.

In the hydrogen scenarios, the conversion efficiency from RES to hydrogen delivery (Well-to-Vehicle efficiency) is 60%, accounting for losses from water electrolysis (65% efficiency) and hydrogen compression. Including the fuel cell conversion in FCEV buses, the overall efficiency (Well-to-Wheels efficiency) drops to 27%. In contrast, for the BEV mobility case, the well-to-wheels efficiency is 65%, encompassing losses related to BESS efficiency and self-discharge (75% efficiency), as well as the round-trip efficiency of the vehicle's battery.

Finally, the self-consumption (Self-cons.) and self-sufficiency (Self-suff.) metrics have been computed. Self-consumption represents the percentage of energy generated from RES used to meet the load, while self-sufficiency describes the share of the load satisfied by RES. In these scenarios, self-sufficiency is 100% as the model is designed to meet the entire load with RES power.

The optimal sizing of the key components for these three scenarios is showcased in Fig. 4.

One of the most notable distinctions between the hydrogen and electric infrastructure lies in the scale of the RES generation plant. In both H_2LoadSet and H_2LoadOpt hydrogen scenarios, the total RES (PV and wind) installed capacity is 3 times the size of the EVLoadSet case. This substantial difference arises from the need to ensure a continuous hydrogen supply throughout the year. The hydrogen generation plant is intentionally oversized to meet this requirement, resulting in the minimum hydrogen storage level occurring on the 2nd of September (week 35), when hydrogen reserves dip to 65 kWh and 70 kWh in the H_2LoadOpt and H_2LoadSet scenarios, respectively. In the H_2Load scenarios, the PV plant is designed to operate at its maximum installable capacity of 104 kW, while the wind plant exceeds the size of

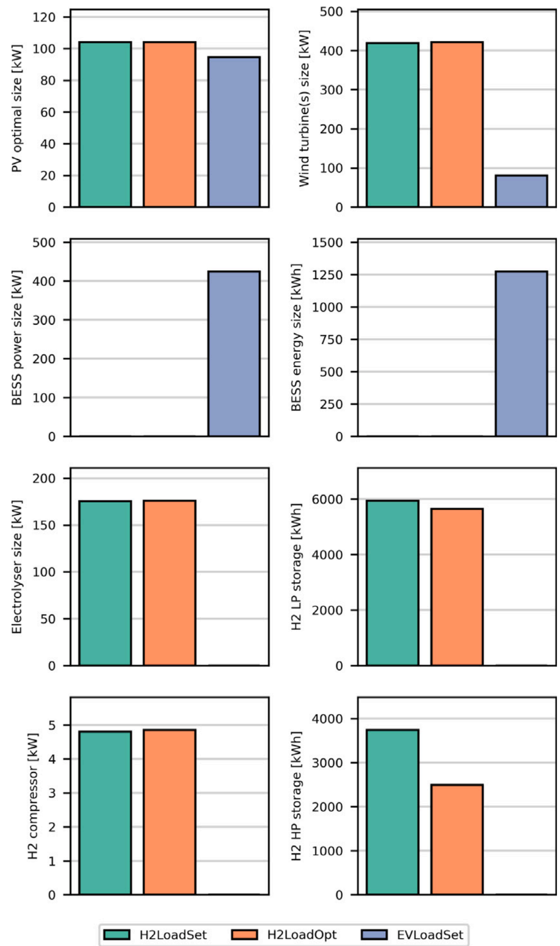

Fig. 4. Optimal size of the hydrogen and electric mobility infrastructure.

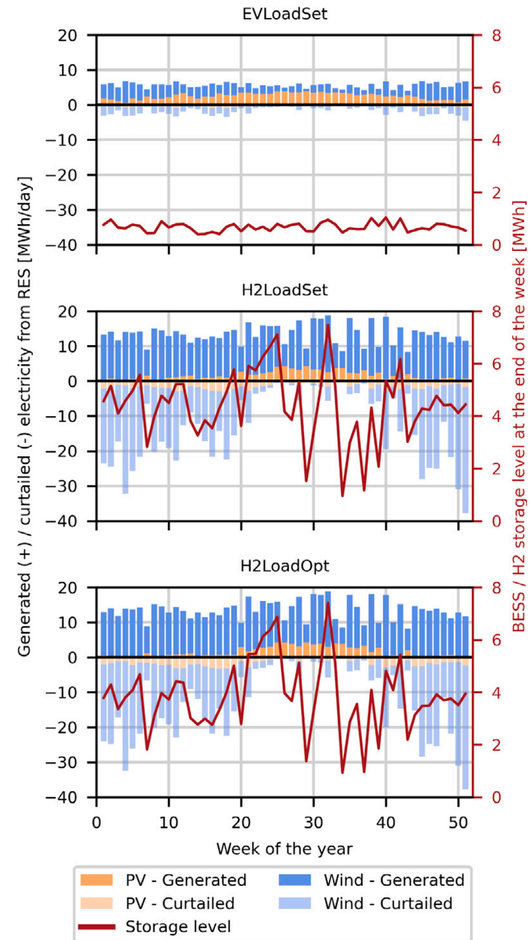

Fig. 5. Electricity generated and curtailed from RES (primary axis) and energy storage level at the end of the week (secondary axis).

the EVLoadSet case by 5.2 times. The maximum capacity of the PV plant is constrained by the available rooftop space of the reference building. This limitation necessitates a larger increase in the installed capacity of the wind power plant to ensure adequate energy production, particularly during summer months when wind generation is lower than in winter months and load requirements are higher. Additionally, prioritizing a higher PV capacity would be preferable due to its lower investment cost per kW and the ability to meet summer load demands without significant curtailment during winter. As depicted in Fig. 5, the energy generated during the summer period (weeks 20–40) is almost entirely consumed, leaving only minimal surplus energy production.

While there is potential to enhance hydrogen generation during the winter months when the energy surplus is greater, this would entail the installation of larger units for hydrogen generation, including electrolyzers, compression, and storage components, incurring elevated capital and operational costs. Consequently, the optimization strategy favors oversizing the generation plants over the hydrogen generation unit.

The high-pressure storage unit for the H_2LoadOpt scenario is approximately 35% smaller compared to the H_2LoadSet scenario. This volume reduction is due to a more evenly distributed bus refueling schedule throughout the day.

We also consider an alternative scenario for hydrogen mobility, which involves integrating a battery energy storage system to potentially reduce the size of the generation plant. However, our optimization efforts reveal that the inclusion of the battery does not yield significant cost savings, resulting in an optimal size of 0 kW.

Conversely, the EVLoadSet scenario demonstrates better adaptability to energy production fluctuations, requiring less energy generation to meet energy demand and subsequently reducing surplus energy or curtailment throughout the year.

The total annualized cost (TAC) refers to the annualized capital and operational costs. As depicted in Fig. 6 (right) the TAC is 177 k€/year for the H_2LoadSet scenario and 172 k€/year for the H_2LoadOpt scenario. In contrast, the annualized cost for the EVLoadSet case is 110 k€/year, approximately 40% lower. Despite the capital cost of hydrogen production components is comparable to that of BESS, the investment cost for RES generation is indeed nearly 3.5 times higher.

However, the electricity overgeneration of the H_2LoadSett and H_2LoadOpt scenarios Fig. 6 (*left*) leads to higher revenues because of the higher amount of electricity injected into the grid, resulting in the LCOD of the H_2 scenarios being 20% lower than in the EVLoadSet scenario, at 0.38–0.40 €/km compared to 0.5 €/km. These values align with the driving cost of diesel-powered buses. Indeed, the average price of diesel in Pantelleria in 2023 was 2.2 €/l and the bus consumption is assumed to be 24 l/100 km, resulting in a driving cost of 0.52 €/km [82] .

These results indicate that while electric mobility is economically more advantageous compared to hydrogen mobility in terms of investment costs, the oversizing of the generation plant, required in the hydrogen case to meet the demand throughout the year, ensures that the LCOD for hydrogen vehicles is lower than that for electric vehicles due to the revenues from the electricity fed into the grid.

Kavadias et al. [24] reported a LCOD of 0.24 €/km for an HRS designed for 25 FCEVs chargings per day. This value is lower than our

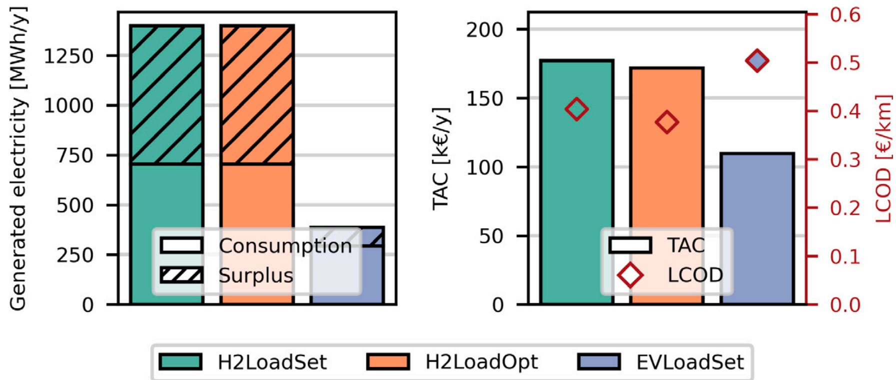

Fig. 6. Economic indicators: (i) electricity consumption and surplus (*left*); (ii) total annualized cost (TAC) and levelized cost of driving (LCOD) (*right*).

Table 7
MCDM performance indices.

Strategies	GHG emitted	LCOD
H_2LoadOpt	1.302 $tn\,CO_{2eq}$ [a]	0.38 €/km
H_2LoadSet	1.302 $tn\,CO_{2eq}$ [a]	0.40 €/km
EVLoadSet	1.919 $tn\,CO_{2eq}$ [a]	0.50 €/km

[a] Values calculated for the average daily energy consumption according to Bionaz et al. [85].

Table 8
MCDM scoring based on economic and environmental criteria.

Strategies	V_i	Position
H_2LoadOpt	1	1
H_2LoadSet	0.914	2
EVLoadSet	0	3

Table 9
MCDM scoring based on economic, energetic and environmental criteria.

Strategies	V_i	Position
H_2LoadOpt	0.216	2
H_2LoadSet	0.208	3
EVLoadSet	0.784	1

findings even if we exclude the costs associated with components for RES generation and the revenues generated from injecting electricity into the grid. Xu et al. [26] and Brown et al. [28] documented an HRS cost of 7.7–19 €/kg for a daily capacity of 100–180 kg. These figures align with our results, which are approximately 6 €/kg. Notably, in these two previous studies, hydrogen was produced through steam methane reforming.

Meanwhile, the cost of BEVs charging stations is assessed by Lanz et al. [83], who estimated the levelized cost of charging in Italy to range between 0.34 and 0.37 €/kWh. It is important to note that their analysis included the installation costs of photovoltaic (PV) systems but assumed the absence of battery storage at the charging site. Conversely, Horesh et al. [84] evaluated the levelized cost of charging for BEVs in the USA, demonstrating that the cost of a 50 kW direct current fast charging station ranged from 0.42 to 0.68 $/kWh for utility ownership. These results closely align with our findings of 0.4 €/kWh (excluding RES generation and electricity revenues).

From the perspective of a decision-maker, for instance, the local administration of Pantelleria, previously discussed scenarios have both advantages and disadvantages as well. The MCDM approach exposed previously can provide an overview of the scenarios investigated.

The evaluation criteria adopted reflect economic and environmental issues. The LCOD has been considered as the economic effort that the policymaker must assume. On the other hand, the GHG emitted represents an environmental criterion that quantifies the carbon footprint of the production side of each technology. According to Fig. 1 and the Fig. 2, the equivalent CO_2 emitted has been evaluated considering the respective storage systems (see Table 7).

By applying the methods detailed in Section 2.4, the objectives weights, calculated according to Eq. (9), indicate a balanced scenario where equivalent CO_2 and LCOD scores are 52% and 48%, respectively. Obtained the objective weights, according to the TOPSIS method, it is possible to calculate the closeness index V_i and establish the overall ranking, as reported in Table 8.

H_2LoadOpt demonstrates superior performance when considering economic and emission parameters. However, including energy parameters, such as well-to-wheels efficiency, can shift the MCDM performance indices in favor of the EV scenarios. In this context, the objective weights are 25% for GHG emissions, 24% for LCOD, and 51% for the well-to-wheels parameter, as shown in Table 9.

Therefore, while the MCDM method is a valuable tool for supporting policymakers' decisions, these decisions should not rely solely on the indices provided. It is crucial to also consider additional factors, such as the intended pathways and long-term strategies for sustainable development in road transport.

Given the limited number of vehicles considered in this study (seven mini-buses), a hybrid solution incorporating both electric and hydrogen vehicles was not analyzed. The investment costs associated with establishing separate infrastructures would significantly impact the project's economic viability. However, if a larger number of users would be considered, exploring this solution becomes intriguing, as economies of scale could potentially mitigate the cost burden. Moreover, exploring sector coupling and microgrid integration among electricity, heating, and transportation could play a pivotal role in reducing storage requirements, maximizing the utilization of renewable resources, and reducing energy costs, especially in island contexts [86–88].

5. Conclusion

This study has examined the feasibility of implementing hydrogen and electric mobility infrastructures for public transportation on an off-grid Mediterranean Italian island. We assessed resource availability for renewable energy plants, optimized infrastructure configurations using PyPSA, and evaluated techno-economic parameters for three distinct scenarios for hydrogen and BEVs mobility. Our results underscore a trade-off between hydrogen and BEV infrastructure. Hydrogen mobility boasts advantages with a lower LCOD of 0.4 €/km and reduced carbon emissions of 1.3 $tn\,CO_{2eq}$. However, BEVs infrastructure proves to be more energy-efficient solution, with a well-to-wheels efficiency of 65%, despite having a higher LCOD at 0.50 €/km and greater carbon emissions of 1.9 $tn\,CO_{2eq}$.

It is worth noting that the LCOD is favorably influenced by the surplus energy injected into the grid, which is significantly higher in the hydrogen scenarios due to the oversized renewable energy generation plant. This design avoids the need for larger hydrogen generation and storage units.

The decision-making process for selecting the most suitable mobility infrastructure should strike a balance between economic, energetic, and environmental considerations.

CRediT authorship contribution statement

Elena Rozzi: Writing – review & editing, Writing – original draft, Visualization, Methodology, Investigation. **Enrico Giglio:** Writing – review & editing, Software, Methodology, Investigation. **Claudio Mosconoli:** Writing – review & editing, Methodology, Investigation, Conceptualization. **Riccardo Novo:** Writing – review & editing, Visualization, Methodology. **Giuliana Mattiazzo:** Writing – review & editing, Supervision, Conceptualization. **Andrea Lanzini:** Writing – review & editing, Supervision, Conceptualization.

Declaration of competing interest

The authors declare that they have no known competing financial interests or personal relationships that could have appeared to influence the work reported in this paper.

Acknowledgment

We would like to acknowledge the valuable contribution of Marco Mungiovì, whose work during his master's thesis laid the foundation for this study.

References

[1] IEA. Electric vehicles. 2022, https://www.iea.org/reports/electric-vehicles. [Accessed 28 August 2023].
[2] Parikh Ahan, Shah Manan, Prajapati Mitul. Fuelling the sustainable future: a comparative analysis between battery electrical vehicles (BEV) and fuel cell electrical vehicles (FCEV). Environ Sci Pollut Res 2023;30(20):57236–52.
[3] Hussein Noon, Massoud Ahmed. Electric vehicle fast chargers: Futuristic vision, market trends and requirements. In: 2019 2nd international conference on smart grid and renewable energy. SGRE, 2019, p. 1–6.
[4] IEA. Electric cars fend off supply challenges to more than double global sales. 2022, https://www.iea.org/commentaries/electric-cars-fend-off-supply-challenges-to-more-than-double-global-sales. [Accessed 28 August 2023].
[5] IEA. Global EV outlook 2022: securing supplies for an electric future. Technical report, IEA; 2022.
[6] IEA. Global EV data explorer. 2023, https://www.iea.org/data-and-statistics/data-tools/global-ev-data-explorer. [Accessed 28 August 2023].
[7] FCH JU. Development of business cases for fuel cells and hydrogen applications for European regions and cities. 2017.
[8] IEA. Fuel cell electric vehicle stock and hydrogen refuelling stations by region. 2021, https://www.iea.org/data-and-statistics/charts/fuel-cell-electric-vehicle-stock-and-hydrogen-refuelling-stations-by-region-2021. [Accessed 28 August 2023].
[9] IEA. Fuel cell electric vehicle stock by region and by mode. 2021, [Accessed 28 August 2023].
[10] IEA. Share of electric and fuel-cell vehicles in total cars and light trucks sales in the sustainable development scenario and net zero emissions by 2050 case, 2019–2030. 2020, [Accessed 28 August 2023].
[11] Szałek Andrzej, Pielecha Ireneusz, Cieslik Wojciech. Fuel cell electric vehicle (FCEV) energy flow analysis in real driving conditions (RDC). Energies 2021;14(16). URL https://www.mdpi.com/1996-1073/14/16/5018.
[12] Wang Zhenpo. Fuel cell electric vehicles (FCEVs). In: Annual report on the big data of new energy vehicle in China (2021). Singapore: Springer Nature Singapore; 2023, p. 135–48.
[13] Sanguesa Julio A, Torres-Sanz Vicente, Garrido Piedad, Martinez Francisco J, Marquez-Barja Johann M. A review on electric vehicles: Technologies and challenges. Smart Cities 2021;4(1):372–404, URL https://www.mdpi.com/2624-6511/4/1/22.
[14] FCH JU. Hydrogen roadmap europe: a sustainable pathway for the European energy transition. 2019.
[15] Shen Zuo-Jun Max, Feng Bo, Mao Chao, Ran Lun. Optimization models for electric vehicle service operations: A literature review. Transp Res B 2019;128:462–77, URL https://www.sciencedirect.com/science/article/pii/S0191261518304545.
[16] Verzijlbergh Remco A, Ilić Marija D, Lukszo Zofia. The role of electric vehicles on a green island. In: 2011 North American power symposium. 2011, p. 1–7.
[17] Işik Uğur Mert, Tercan Said Mirza, Gökalp Erdin. Optimal sizing and detailed analysis of microgrid with photovoltaic panel and battery energy storage system integrated electric vehicle charging station. In: 2023 5th international congress on human-computer interaction, optimization and robotic applications. HORA, 2023, p. 1–9.
[18] Nafeh Abd El-Shafy A, Omran Abd El-Fattah A, Elkholy A, Yousef HosamKM. Optimal economical sizing of a PV-battery grid-connected system for fast charging station of electric vehicles using modified snake optimization algorithm. Results Eng 2024;21:101965, URL https://www.sciencedirect.com/science/article/pii/S2590123024002184.
[19] Zhao Xunwen, Mu Hailin, Li Nan, Shi Xunpeng, Chen Chaonan, Wang Hongye. Optimization and analysis of an integrated energy system based on wind power utilization and on-site hydrogen refueling station. Int J Hydrog Energy 2023;48(57):21531–43, URL https://www.sciencedirect.com/science/article/pii/S0360319923010704.
[20] Barhoumi El Manaa, Okonkwo Paul C, Zghaibeh Manaf, Belgacem Ikram Ben, Farhani Slah, Bacha Faouzi. Optimization of PV-grid connected system based hydrogen refueling station. In: 2022 8th international conference on control, decision and information technologies. CoDIT, Vol. 1, 2022, p. 1603–7.
[21] Barhoumi El Manaa, Salhi Mohamed Salah, Okonkwo Paul C, Ben Belgacem Ikram, Farhani Slah, Zghaibeh Manaf, Bacha Faouzi. Techno-economic optimization of wind energy based hydrogen refueling station case study salalah city oman. Int J Hydrog Energy 2023;48(26):9529–39, URL https://www.sciencedirect.com/science/article/pii/S0360319922058670.
[22] Ibáñez-Rioja Alejandro, Järvinen Lauri, Puranen Pietari, Kosonen Antti, Ruuskanen Vesa, Hynynen Katja, Ahola Jero, Kauranen Pertti. Off-grid solar PV–wind power–battery–water electrolyzer plant: Simultaneous optimization of component capacities and system control. Appl Energy 2023;345:121277, URL https://www.sciencedirect.com/science/article/pii/S0306261923006414.
[23] Schröder M, Abdin Z, Mérida W. Optimization of distributed energy resources for electric vehicle charging and fuel cell vehicle refueling. Appl Energy 2020;277:115562, URL https://www.sciencedirect.com/science/article/pii/S0306261920310746.
[24] Kavadias Kosmas A, Kosmas Vasileios, Tzelepis Stefanos. Sizing, optimization, and financial analysis of a green hydrogen refueling station in remote regions. Energies 2022;15(2). URL https://www.mdpi.com/1996-1073/15/2/547.
[25] Wu Xiong, Zhao Wencheng, Li Haoyu, Liu Bingwen, Zhang Ziyu, Wang Xiuli. Multi-stage stochastic programming based offering strategy for hydrogen fueling station in joint energy, reserve markets. Renew Energy 2021;180:605–15, URL https://www.sciencedirect.com/science/article/pii/S0960148121012428.
[26] Xu Xinhai, Xu Ben, Dong Jun, Liu Xiaotong. Near-term analysis of a roll-out strategy to introduce fuel cell vehicles and hydrogen stations in Shenzhen China. Appl Energy 2017;196:229–37, URL https://www.sciencedirect.com/science/article/pii/S0306261916316336.
[27] Martínez de León C, Ríos C, Brey JJ. Cost of green hydrogen: Limitations of production from a stand-alone photovoltaic system. Int J Hydrog Energy 2023;48(32):11885–98, URL https://www.sciencedirect.com/science/article/pii/S0360319922021280. XII Edition of the International Conference on Hydrogen Production.
[28] Brown Tim, Schell Lori Smith, Stephens-Romero Shane, Samuelsen Scott. Economic analysis of near-term California hydrogen infrastructure. Int J Hydrog Energy 2013;38(10):3846–57, URL https://www.sciencedirect.com/science/article/pii/S0360319913002346.
[29] Brown T, Hörsch J, Schlachtberger D. PyPSA: Python for power system analysis. J Open Res Softw 2018;6(4). arXiv:1707.09913.
[30] Danielis Romeo, Scorrano Mariangela, Giansoldati Marco. Decarbonising transport in europe: Trends, goals, policies and passenger car scenarios. Res Transp Econom 2022;91:101068.
[31] Hwang Ching-Lai, Lai Young-Jou, Liu Ting-Yun. A new approach for multiple objective decision making. Comput Oper Res 1993;20:889–99.
[32] Diakoulaki D, Mavrotas G, Papayannakis L. Determining objective weights in multiple criteria problems: The critic method. Comput Oper Res 1995;22:763–70.
[33] Caponi Roberta, Ferrario Andrea Monforti, Bocci Enrico, Bødker Sandra, del Zotto Luca. Single-tank storage versus multi-tank cascade system in hydrogen refueling stations for fuel cell buses. Int J Hydrog Energy 2022;47(64):27633–45, URL https://www.sciencedirect.com/science/article/pii/S0360319922027124.
[34] Li Xianming Jimmy, Allen Jeffrey D, Stager Jerad A, Ku Anthony Y. Paths to low-cost hydrogen energy at a scale for transportation applications in the USA and China via liquid-hydrogen distribution networks. Clean Energy 2020;4(1):26–47, arXiv:https://academic.oup.com/ce/article-pdf/4/1/26/33004905/zkz033.pdf.
[35] Bai Yunfeng, Zhang Caizhi, Duan Hao, Jiang Shangfeng, Zhou Zhiming, Grouset Didier, Zhang Mingjun, Ye Xuefeng. Modeling and optimal control of fast filling process of hydrogen to fuel cell vehicle. J Energy Storage 2021;35:102306, URL https://www.sciencedirect.com/science/article/pii/S2352152X21000694.
[36] Lindberg Fredrik, Jonsson Per, Honjo Tsuyoshi, Wästberg Dag. Solar energy on building envelopes – 3D modelling in a 2D environment. Sol Energy 2015;115:369–78, URL https://www.sciencedirect.com/science/article/pii/S0038092X15001164.

[37] QGIS geographic information system. 2023, https://www.qgis.org/it/site/. [Accessed 28 August 2023].
[38] Moscoloni Claudio, Zarra Fernando, Novo Riccardo, Giglio Enrico, Vargiu Alberto, Mutani Guglielmina, Bracco Giovanni, Mattiazzo Giuliana. Wind turbines and rooftop photovoltaic technical potential assessment: Application to sicilian minor islands. Energies 2022;15(15). URL https://www.mdpi.com/1996-1073/15/15/5548.
[39] Lindberg Fredrik, Grimmond CSB, Gabey Andrew, Jarvi Leena, Kent Christoph W, Krave Niklas, Sun Ting, Wallenberg Helena, Ward Helen C. Urban multi-scale environmental predictor (UMEP) manual. 2019, URL https://umep-docs.readthedocs.io/.
[40] Autodesk. AutoCAD overview. 2023, https://www.autodesk.it/products/autocad. [Accessed 28 August 2023].
[41] JRC. PVGIS. 2023, https://joint-research-centre.ec.europa.eu/photovoltaic-geographical-information-system-pvgis/getting-started-pvgis/pvgis-user-manual_en. [Accessed 28 August 2023].
[42] WASP. 2023, https://www.wasp.dk/wasp. [Accessed 28 August 2023].
[43] Renewables.ninja. 2023, https://www.renewables.ninja/. [Accessed 28 August 2023].
[44] Cplex and IBM ILOG. V20. 1 . 1: User's manual for CPLEX. Int Bus Mach Corp 2021.
[45] NETL. Quality guidelines for energy system studies: cost estimation methodology for NETL assessments of power plant performance. Final report DOE/NETL-2011/1455, National Energy Technology Laboratory, Office of Program Performance & Benefits, Performance Division; 2011, URL http://www.netl.doe.gov.
[46] Minutillo M, Perna A, Forcina A, Di Micco S, Jannelli E. Analyzing the levelized cost of hydrogen in refueling stations with on-site hydrogen production via water electrolysis in the Italian scenario. Int J Hydrog Energy 2021;46(26):13667–77, URL https://www.sciencedirect.com/science/article/pii/S0360319920343160. European Fuel Cell Conference & Exhibition 2019.
[47] Broniewicz Elzbieta, Ogrodnik Karolina. Multi-criteria analysis of transport infrastructure projects. Transp Res D 2020;83:102351, URL https://www.sciencedirect.com/science/article/pii/S1361920920305381.
[48] Broniewicz Elzbieta, Ogrodnik Karolina. A comparative evaluation of multi-criteria analysis methods for sustainable transport. Energies 2021;14(16). URL https://www.mdpi.com/1996-1073/14/16/5100.
[49] Hassan Imad, Alhamrouni Ibrahim, Azhan Nurul Hanis. A CRITIC-TOPSIS multi-criteria decision-making approach for optimum site selection for solar PV farm. Energies 2023;16(10). URL https://www.mdpi.com/1996-1073/16/10/4245.
[50] Mukhametzyanov Irik. Specific character of objective methods for determining weights of criteria in MCDM problems: Entropy, CRITIC and SD. Decis Mak: Appl Manage Eng 2021;4:76–105.
[51] Chakraborty Subrata. TOPSIS and modified TOPSIS: A comparative analysis. Decis Anal J 2022;2:100021, URL https://www.sciencedirect.com/science/article/pii/S277266222100014X.
[52] Novo Riccardo, Minuto Francesco Demetrio, Bracco Giovanni, Mattiazzo Giuliana, Borchiellini Romano, Lanzini Andrea. Supporting decarbonization strategies of local energy systems by de-risking investments in renewables: A case study on pantelleria island. Energies 2022;15(3). URL https://www.mdpi.com/1996-1073/15/3/1103.
[53] Marsala travel bus. 2023, https://www.marsalatravelbus.it/. [Accessed 28 August 2023].
[54] Lubecki Adrian, Szczurowski Jakub, Zarębska Katarzyna. A comparative environmental life cycle assessment study of hydrogen fuel, electricity and diesel fuel for public buses. Appl Energy 2023;350:121766, URL https://www.sciencedirect.com/science/article/pii/S0306261923011303.
[55] Rout Cameron, Li Hu, Dupont Valerie, Wadud Zia. A comparative total cost of ownership analysis of heavy duty on-road and off-road vehicles powered by hydrogen, electricity, and diesel. Heliyon 2022;8(12):e12417, URL https://www.ncbi.nlm.nih.gov/pmc/articles/PMC9803793/. PMID: 36593823.
[56] Rampini - SIXTRON. 2023, https://www.rampini.it/it/autobus-mezzi-speciali_4/prodotti/sixtron-e-bus-autobus-elettrico-rampini_100/. [Accessed 28 August 2023].
[57] Dolomitech - progettazione e prodotti. 2023, https://www.dolomitech.com/progettazione-e-prodotti/. [Accessed 28 August 2023].
[58] Jinko solar - tiger neo. 2023, https://jinkosolar.eu/products/tiger-neo/. [Accessed 28 August 2023].
[59] International Renewable Energy Agency. Renewable power generation costs in 2021. Technical report, Abu Dhabi: IRENA; 2022.
[60] National Renewable Energy Laboratory. 2023 annual technology baseline. Technical report, Golden, CO: NREL; 2023, URL https://atb.nrel.gov/.
[61] Martínez de León C, Ríos C, Brey JJ. Cost of green hydrogen: Limitations of production from a stand-alone photovoltaic system. Int J Hydrog Energy 2023;48(32):11885–98, URL https://www.sciencedirect.com/science/article/pii/S0360319922021280. XII Edition of the International Conference on Hydrogen Production.
[62] Sens Lucas, Neuling Ulf, Kaltschmitt Martin. Capital expenditure and levelized cost of electricity of photovoltaic plants and wind turbines – development by 2050. Renew Energy 2022;185:525–37, URL https://www.sciencedirect.com/science/article/pii/S0960148121017626.
[63] Ziegler Lisa, Gonzalez Elena, Rubert Tim, Smolka Ursula, Melero Julio J. Lifetime extension of onshore wind turbines: A review covering Germany, Spain, Denmark, and the UK. Renew Sustain Energy Rev 2018;82:1261–71, URL https://www.sciencedirect.com/science/article/pii/S1364032117313503.
[64] Saba Sayed M, Müller Martin, Robinius Martin, Stolten Detlef. The investment costs of electrolysis – A comparison of cost studies from the past 30 years. Int J Hydrog Energy 2018;43(3):1209–23, URL https://www.sciencedirect.com/science/article/pii/S0360319917344956.
[65] Buttler Alexander, Spliethoff Hartmut. Current status of water electrolysis for energy storage, grid balancing and sector coupling via power-to-gas and power-to-liquids: A review. Renew Sustain Energy Rev 2018;82:2440–54, URL https://www.sciencedirect.com/science/article/pii/S136403211731242X.
[66] Rozzi Elena, Minuto Francesco Demetrio, Lanzini Andrea. Dynamic modeling and thermal management of a power-to-power system with hydrogen storage in microporous adsorbent materials. J Energy Storage 2021;41:102953, URL https://www.sciencedirect.com/science/article/pii/S2352152X2100668X.
[67] Martínez de León C, Ríos C, Brey JJ. Cost of green hydrogen: Limitations of production from a stand-alone photovoltaic system. Int J Hydrog Energy 2023;48(32):11885–98, URL https://www.sciencedirect.com/science/article/pii/S0360319922021280. XII Edition of the International Conference on Hydrogen Production.
[68] Lee Hyunjun, Lee Boreum, Byun Manhee, Lim Hankwon. Economic and environmental analysis for PEM water electrolysis based on replacement moment and renewable electricity resources. Energy Convers Manage 2020;224:113477, URL https://www.sciencedirect.com/science/article/pii/S0196890420310098.
[69] International Renewable Energy Agency. Green hydrogen cost reduction: Scaling up electrolysers to meet the 1.5 °C climate goal. Technical report, Abu Dhabi: International Renewable Energy Agency, IRENA; 2020.
[70] Bareiß Kay, de la Rua Cristina, Möckl Maximilian, Hamacher Thomas. Life cycle assessment of hydrogen from proton exchange membrane water electrolysis in future energy systems. Appl Energy 2019;237:862–72, URL https://www.sciencedirect.com/science/article/pii/S0306261919300017.
[71] Caponi Roberta, Bocci Enrico, Del Zotto Luca. Techno-economic model for scaling up of hydrogen refueling stations. Energies 2022;15(20). URL https://www.mdpi.com/1996-1073/15/20/7518.
[72] Xu Xinhai, Xu Ben, Dong Jun, Liu Xiaotong. Near-term analysis of a roll-out strategy to introduce fuel cell vehicles and hydrogen stations in Shenzhen China. Appl Energy 2017;196:229–37, URL https://www.sciencedirect.com/science/article/pii/S0306261916316336.
[73] FCH-JU. Study on early business cases for H2 in energy storage and more broadly power to H2 applications. Final report, Brussels, Belgium: FCH-JU; 2017, Client: FCH-JU, Project: EARLY BUSINESS CASES FOR H2 IN ENERGY STORAGE AND MORE BROADLY POWER TO H2 APPLICATIONS.
[74] Katikaneni Sai P, Al-Muhaish Fahad, Harale Aadesh, Pham Thang V. On-site hydrogen production from transportation fuels: An overview and techno-economic assessment. Int J Hydrog Energy 2014;39(9):4331–50, URL https://www.sciencedirect.com/science/article/pii/S0360319913031649.
[75] Caponi Roberta, Ferrario Andrea Monforti, Bocci Enrico, Juelsgaard Kristina Fløche. Four years of operational data for five hydrogen refueling stations. E3S Web Conf 2022;334:06008.
[76] Update of the remuneration due, pursuant to resolution 558/2018/r/EFR, in the case of energy production plants from renewable sources built on non-interconnected islands that come into operation starting from january 1, 2019. 2018.
[77] Giglio Enrico, Luzzani Gabriele, Terranova Vito, Trivigno Gabriele, Niccolai Alessandro, Grimaccia Francesco. An efficient artificial intelligence energy management system for urban building integrating photovoltaic and storage. IEEE Access 2023;11:18673–88.
[78] Kebede Abraham Alem, Kalogiannis Theodoros, Van Mierlo Joeri, Berecibar Maitane. A comprehensive review of stationary energy storage devices for large scale renewable energy sources grid integration. Renew Sustain Energy Rev 2022;159:112213, URL https://www.sciencedirect.com/science/article/pii/S1364032122001368.
[79] Grimaldi Alberto, Minuto Francesco Demetrio, Perol Alessandro, Casagrande Silvia, Lanzini Andrea. Ageing and energy performance analysis of a utility-scale lithium-ion battery for power grid applications through a data-driven empirical modelling approach. J Energy Storage 2023;65:107232, URL https://www.sciencedirect.com/science/article/pii/S2352152X23006291.
[80] Giglio Enrico, Novo Riccardo, Mattiazzo Giuliana, Fioriti Davide. Reserve provision in the optimal planning of off-grid power systems: Impact of storage and renewable energy. IEEE Access 2023;11:100781–97.
[81] Nicholas Michael. Estimating electric vehicle charging infrastructure costs across major U.S. metropolitan areas. Working paper 2019–14, International Council on Clean Transportation; 2019.
[82] Al-Mahadin Aziz, Mustafa Mohamad Y. Utilizing fuel cell technology for dubai roads and transport authority (RTA). 2018, p. 1–6.
[83] Lanz Lukas, Noll Bessie, Schmidt Tobias S, Steffen Bjarne. Comparing the levelized cost of electric vehicle charging options in europe. Nature Commun 2022;13(1):5277.

[84] Horesh Noah, Zhou Yan, Quinn Jason. Home charging for all: Techno-economic and life cycle assessment of multi-unit dwelling electric vehicle charging hubs. J Clean Prod 2023;383:135551, URL https://www.sciencedirect.com/science/article/pii/S0959652622051253.

[85] Bionaz David, Marocco Paolo, Ferrero Domenico, Sundseth Kyrre, Santarelli Massimo. Life cycle environmental analysis of a hydrogen-based energy storage system for remote applications. Energy Rep 2022;8:5080–92.

[86] Dorotić Hrvoje, Doračić Borna, Dobravec Viktorija, Pukšec Tomislav, Krajačić Goran, Duić Neven. Integration of transport and energy sectors in island communities with 100. Renew Sustain Energy Rev 2019;99:109–24, URL https://www.sciencedirect.com/science/article/pii/S1364032118306816.

[87] Babaei Reza, Ting David S-K, Carriveau Rupp. Optimization of hydrogen-producing sustainable island microgrids. Int J Hydrog Energy 2022;47(32):14375–92, URL https://www.sciencedirect.com/science/article/pii/S0360319922008242.

[88] Gay Destine, Rogers Tom, Shirley Rebekah. Small island developing states and their suitability for electric vehicles and vehicle-to-grid services. Util Policy 2018;55:69–78, URL https://www.sciencedirect.com/science/article/pii/S0957178718300730.